Post-saccadic following in the marmoset monkey as a read-out of pre-saccadic attention

Shanna H. Coop[1], Garrett W. Bunce[2], Yonatan T. Abrham[1], Amy Bucklaew[1], Jude F. Mitchell[1]*

[1]Department of Brain and Cognitive Sciences, University of Rochester, Rochester NY
[2] Department of Pharmacology, University of Maryland, Baltimore
* Correspondence to: jmitch27@ur.rochester.edu

Abstract

Primates move their eyes 2-3 times per second to bring objects of interest to central, high-resolution vision. For moving objects, they use a combination of rapid saccadic eye movements along with smooth following movements to track targets continuously. Eye movements produce perceptual enhancements for the saccade target, called pre-saccadic attention. Recently, we found in humans that saccades to peripheral motion apertures resulted in smooth post-saccadic following of stimulus motion (Kwon et al, 2019). The early phase of post-saccadic following reflects motion integration at the target before the saccade and could provide a behavioral read-out of the target's motion. Here we examined post-saccadic following in marmoset monkeys. Marmosets performed a saccade foraging task in which they made a saccade to one of three different motion apertures. Immediately upon saccade offset, the marmoset's eye movements followed the target's motion with a low (10-20%) gain that was consistent with what has been observed in humans. The motion from other non-target apertures also influenced following responses, though with much weaker gain. The gain was distributed equally across apertures before the saccade but enhanced for the target immediately after the saccade, consistent with a post-saccadic enhancement (Gardner and Lisberger, 2001). This following response provided an estimate of target motion with a median absolute angular error of roughly 40 degrees, half as accurate as explicitly trained reports (Cloherty et. al., 2020). Further, the relative gain for the target motion direction versus other apertures provided an index of attentional selection. Thus smooth eye movements provide a read-out both of pre-saccadic motion integration and attention.

New & Noteworthy

Using a saccade foraging paradigm in marmoset monkeys we measured visual motion integration and pre-saccadic attention from smooth following eye movements with minimal animal training.

Introduction

Our visual system deals with a wealth of visual information entering the eyes. We make saccadic eye movements to sample the visual world to ensure high acuity across the visual field. Each saccade produces perceptual enhancements before the eyes move, called pre-saccadic attention (Henderson et al. 1989, Kowler, Anderson, Dosher, & Blaser, 1995; Deubel & Schneider, 1996; Rolfs et al., 2011; White et al., 2013). Pre-saccadic attention has been studied extensively in human psychophysics and shown to improve orientation sensitivity and perceived contrasts for targets (Rolfs & Carrasco, 2012; Ohl, Kuper, & Rolfs, 2017), as well as increase sensitivity for high spatial frequency features (Li, Barbot, & Carrasco, 2016). This happens in an incredibly rapid timeframe, with perceptual enhancements occurring only 50-100 ms before the saccade (Deubel, 2008; Li et al., 2016; Ohl et al., 2017; Rolfs & Carrasco, 2012; Rolfs et al., 2011). These increases in sensitivity have also been found to be automatic and obligatory with every saccade, meaning that it occurs even if it impairs task performance (Deubel, 2008; Montagnini & Castet, 2007).

A recent study found that pre-saccadic attention recruits smooth eye movements automatically (Kwon, Rolfs & Mitchell, 2019). Eye movements immediately following a saccade to a motion stimulus were found to track the motion, even though the task discouraged tracking, and the effect persisted even if the stimulus disappeared during saccade flight. The removal of the stimulus in saccade flight demonstrates that the post-saccadic following response (PFR) relies on pre-saccadic motion information, and is not directly driven by motion observed at the fovea in the post-saccadic period. By focusing on the early “open-loop” period (20-100ms) after the saccade offset, they found that they could isolate the effect of peripheral motion on the PFR and provide a behavioral read-out of its direction. While most psychophysical studies have used perceptual or saccadic reports of peripheral stimuli to measure pre-saccadic attention, the PFR provides a simple behavioral read-out for motion stimuli. Such an automatic read-out could be highly valuable in animal studies for correlating behavior to neuronal effects, as it would not require extensive training to make saccadic reports of motion direction.

In the current study, we examined post-saccadic smooth eye movements in the marmoset monkey, a small-bodied New World species. The marmoset monkey offers several advantages as a model for visual neuroscience (Mitchell & Leopold 2015). Among primates, the marmoset is specialized for its smaller size and rapid breeding, but also has a visual system that is highly similar in organization to that of larger species like the macaque (Mitchell & Leopold 2015; Solomon & Rosa 2014). Furthermore, the marmoset is an ideal candidate for modern imaging and array recording techniques because nearly all of its visual and oculomotor cortical areas lie accessible on the smooth surface of its lissencephalic brain (Chaplin et al., 2017; Zavitz et al., 2017). Marmosets also have a specialized fovea with comparably high cone density to other primates (Troilo, Rowland, & Judge, 1993). Their eye movements and central visual acuity scale with eccentricity similar to other primates, with acuity about half that of larger primates due to the size of their eye (Nummela et al, 2017). Further, they exhibit comparable saccadic eye movements to direct their fovea toward targets (Mitchell et al., 2014) including tracking moving targets in smooth pursuit behavior (Mitchell, Priebe & Miller, 2015). Recently, it has also been

shown that marmosets can be trained to make explicit saccadic reports of motion direction using traditional random dot motion stimuli of varying coherence levels (Cloherty et al., 2019). This study presented motion stimuli at central visual field. and then included an analog report of their perceived direction of motion by a saccade made to a peripheral ring surrounding the stimulus. Although the marmoset performed the task with an angular accuracy in reporting motion direction that was comparable to human participants, it required extensive training over a 6-12 month period. Even after training, marmosets maintained significant lapse rates in the task. Here, we are interested if motion can instead be automatically read out from involuntary following eye movements at saccade offset.

We characterized smooth post-saccadic following responses (PFR) in marmosets trained to perform a simple foraging saccade task where the motion direction of the stimuli was task irrelevant. We measured how well their eye movements tracked a target's motion in the open-loop periods after a saccade to the target aperture. Trials in which the target disappeared during saccade flight were included to verify the following was not driven from post-saccadic foveal motion, and to estimate the open-loop period, which we found was shorter in marmosets than in humans. To estimate the degree of post-saccadic following we computed the gain of following and compared it against the previous study in humans (Kwon et al, 2019). Further, we compute the angular errors of the following vector in the open-loop period to consider to what extent it provides a reliable measure of motion direction and compared it against explicit saccadic reports from a previous study in marmoset monkeys (Cloherty et al., 2020). We find that PFR provides a behavioral readout of peripheral motion integration, which when combined with neurophysiological investigations in marmosets, creates the opportunity to study the neuronal mechanisms of pre-saccadic attention enhancements in motion processing.

Methods

Subjects and Surgery

All experimental protocols were approved by the University of Rochester Institutional Animal Care and Use Committee and were conducted in compliance with the National Institutes of Health guidelines for animal research. Four adult common marmosets (Callithrix jacchus), three males and one female (ages ranging from 2-8 years) participated in a saccade foraging study with eye tracking. Subjects were housed at the University of Rochester with a circadian cycle of 12-hour light and 12-hour dark. Subjects were briefly food scheduled with full access to water during early training to learn how to perform fixation tasks, but afterwards had no food restrictions at the time behavioral data was collected.

All subjects were surgically implanted with head caps to help stabilize them for head-fixed eye tracking. Two months prior to surgery, subjects were trained to sit in a small primate chair following methods previously described (Lu et al. 2001; Remington et al. 2012; Osmanski et al. 2013; Nummela et al. 2017). Then subjects underwent surgery under sterile conditions to implant an acrylic head cap with a titanium post to stabilize the head using methods described in detail previously (Nummela et al., 2017). After a recovery period of about 2-3 weeks,

marmosets were acclimated to head fixing in the primate chair, and then were trained to maintain fixation on a small central point using methods previously described (Mitchell et al., 2014; Nummela et al., 2017). Each marmoset subject underwent initial training over 1-2 months to perform a visual acuity task enabling us to correct their vision for any myopia identified. They performed a center-out saccade to detect a Gabor grating of varying spatial frequency placed at random locations of 5 degrees eccentricity as described previously (Nummela et al, 2017). After learning the task, each subject's vision was then corrected using spherical concave lenses (Optimark Perimeter Lens Set) that were centered 4–5 mm in front of the face. The power of the lens was varied in daily behavioral sessions to identify the lowest power correction that achieved their maximum acuity in the task. The diopters of the lens used for the 4 marmosets in the present study were -1.0, -2.5, -1.5, and -2.0 respectively for marmosets 1-4.

Stimulus presentation and timing

Stimuli were generated using the Psychophysics toolbox (Brainard, 1997; Kleiner et al., 2007; Pelli, 1997) in MATLAB 2015b (MathWorks, Natick, MA) on a windows computer (Intel i7 CPU, Windows 7, 8 GB RAM, GeForce Ti graphics card). They were presented on a gamma-corrected display (BenQ X2411z LED monitor, resolution: 1,920 x 1,080 p, refresh rate: 100Hz, gamma correction: 2.2) that had a dynamic luminance range from 0.5 to 230 cd/m2 at a distance of 57 cm in a dark room and viewed under head-restraint in custom designed primate chair as described previously (Nummela et. al., 2017). Brightness on the BenQ display was set to 100 and contrast to 50, and additional visual features of the monitor, such as blur reduction and low blue light, were turned off. Gamma corrections were verified with measurement by a photometer. Task events and eye movements are recorded using a Datapixx I/O box (Vpixx technologies) for temporal registration. Matlab code is available online (https://github.com/jcbyts/MarmoV5).

Peripheral visual stimuli consisted of random dot motion fields viewed within a Gaussian aperture **(Figure 1A)**. Each aperture contained a field of black dots (each dot with a 0.15 dva diameter with a density of 2.54 dots per visual degree squared) which moved at either 6.75 or 12 dva/s degrees/sec in one direction (100% coherent). Depending on the experimental condition, the dots either had unlimited lifetimes or limited lifetimes of 50ms with asynchronous updating to new locations. The dots appeared in black (0.5cd/m^2) against a grey background (115 cd/m^2). Stimuli were positioned at 5 degrees eccentric locations with a radius of 2.5 degrees and the contrast of dots was decreased from black at the center of the field to zero on the aperture edges according to a Gaussian envelope with a half-width of 1.67 degrees (σ = 0.83 degrees). The motion direction of each aperture was chosen at random and independently from the other apertures selecting from 1 of 16 directions that spanned 0 to 360 degrees in steps of 22.5 degrees.

Eye Tracking

Eye position was acquired either at 220 Hz using an Arrington Eye Tracker with Viewpoint software (Arrington Research) or at 1000 Hz using an Eyelink 1000 Plus eye tracker (SR

research). The eye was imaged under infrared light through a dichroic mirror (part #64-472, Edmunds Optics) placed at a 45-degree angle in front of the observer, allowing for a direct view of the pupil. Each marmoset viewed the screen through a spherical concave lens that was identified to correct any potential myopia, as described above. Eye position data was collected during behavioral sessions and processed to detect eye movements. At the start of each session the eye tracker was calibrated using a face detection task designed to guide fixation for marmosets described previously (Mitchell et al., 2014, Nummela et al. 2017). Raw horizontal and vertical eye position signals were smoothed offline with a median filter (over 5 samples), if collected at 220 Hz upsampled to 1000 Hz by linear interpolation, and then convolved with a Gaussian kernel (5ms half width, out to 3 SD, -15 to 15ms) to minimize high-frequency noise. For offline detection of saccadic eye movements, we used an automatic procedure that detected deviations in 2-D eye velocity space (Engbert & Mergenthaler, 2006; Kwon et al., 2019). We computed horizontal and vertical eye velocity by taking the temporal difference of the smoothed eye-position traces. Saccades were then marked by events where the 2D velocity exceeded the median velocity by 10 SD for at least 15ms (Engbert & Mergenthaler, 2006; Kwon et al., 2019) and events merged into a single event if they were separated by less than 5ms. Saccade onset and offset were determined by the first and last time the 2-D velocity crossed the median velocity threshold. Any trials in which an eye blink occurred were flagged by the abrupt change in eye position to a location outside the visible screen and were removed from the analysis.

Behavioral Task

To study post-saccadic following response (PFR), we had subjects perform a foraging saccade task to peripheral motion apertures **(Figure 1A)**. Each trial began with the fixation of a small bullseye spot (0.3 degree outer radius, 0.5 cd/m^2 center, 230 cd/m^2 surround) for a delay uniformly distributed between 0.1 to 0.3 s, presented on a gray background (115 cd/ m^2). Fixation was maintained within a 1.5 degree radius window around the small spot. After the fixation period, three dot motion apertures appeared in the periphery while the fixation spot was offset. For each trial, the direction of motion of each stimulus was independently sampled from 16 motion directions. The three apertures appeared at 5 degrees eccentricity in one of two configurations across blocks of 20 trials. The first configuration had a single target above fixation along the vertical meridian with two other targets in the lower hemi-fields each spaced on a circle 120 degrees apart, while the second configuration was the vertically flipped form of the first configuration, thus across blocks sampling 6 peripheral locations. Each aperture contained 50 dots windowed within a Gaussian envelope (as described above). Across sessions, we varied both dot speed (6.75 or 12 dva/s) and lifetime (unlimited lifetime or limited lifetime of 50 ms – 5 video frames). We collected behavioral sessions opportunistically on days when marmoset subjects were not involved in other experiments. Each marmoset performed a minimum of 4 sessions (range 4-8) working up to 600 trials using 6.75 dva/s with unlimited lifetime dots were used to make direct comparisons to a previous study in humans (Kwon et al. 2019). Other sessions used 12 dva/s with unlimited and limited lifetime dots interleaved randomly across trials, with marmosets performing a minimum of 6 sessions (range 6-9) working up to 1200 total trials. In three marmoset monkeys we were able to include additional sessions (range 12-21) working up to 600 trials which only displayed limited lifetime dots and varied motion coherence by the bandwidth of motion directions sampled (0°, 90°, 180°, 270°,

360°) with stimuli matched in properties to a previous study with saccadic reports (Cloherty et al, 2020).

Behavioral performance in the foraging task demanded only that marmosets make a saccade to different peripheral apertures across trials to receive liquid rewards. From the onset of apertures, the subject was given up to 1.5 s to make a saccade out of the fixation window to one of the aperture targets and land within a 2.5 degree window around the aperture center. Eye position needed to remain in the aperture for 0.2 s to confirm the saccade endpoint. In 50% of the trials the motion stimuli disappeared during saccade flight, such that in the post-saccadic period no foveal motion was present. Saccades were detected by eye position crossing the fixation window to disappear the stimulus. Across trials we rewarded saccades to any aperture as long it differed from the aperture chosen in the previous trial in order to encourage foraging. It should be noted that the motion directions of the dot apertures were irrelevant to obtaining reward and were selected at random and independent of each other in each trial. A correct choice was rewarded with a 5-10 uL liquid reward and the appearance of a marmoset face at the aperture location after the trial (0.2 s after saccade confirmation) to provide a secondary positive feedback in conjunction with juice reward. The juice reward consisted of marshmallows blended with water that were prepared fresh for each daily session (1-2 large, 60 g, marshmallows blended in 60 mL hot water, left to settle for a few minutes, and then the lower non-foam portion drawn into a 20 cc syringe). An incorrect choice resulted in a black Gaussian spot that filled the aperture location instead of a face as feedback, and no liquid reward, as feedback for choosing a repeated location.

Trial criteria

Trials contaminated by micro-saccades, double-step saccades, or post-saccadic correctional saccades were excluded from analyses. We excluded trials with micro-saccades of amplitude greater than 0.5 visual degrees during the fixation hold period. To ensure that the animal had not initiated a saccade prior to stimulus presentation, we also excluded trials where the reaction time of saccade initiation was under 0.1 sec. We also excluded trials to ensure only a single-step, accurate saccades were made to the aperture. We excluded trials where the animal made two smaller saccades to the aperture (double-step) as opposed to one larger saccade (8.1% of saccade trials). We required that the saccade end-point fell within 2.5 degrees of the aperture center. Last, if a micro-saccade occurred in the 0.2s after the saccade offset the trials were excluded. Overall, this led to removing on average 10.3% (+/- 2.9% sd.) of total trials due to possible contamination from small or inaccurate eye movements. Subsequent analyses only included accurate single step saccades to apertures.

Eye movement analysis

We examined if marmoset eye movements tracked the target motion immediately following the saccade offset. An example 2D eye position trace from one trial illustrates the low gain post-saccadic following movements for motion direction for a saccade to one of the motion dot apertures **(Figure 1C)**. The black dots show the trace of the animal's eye position, while the end of blue arrow indicate the center of one of the motion dot apertures, and the blue arrow's

direction indicates the motion direction of the moving dots in that aperture. We examined an open-loop period from 20ms to 60ms after saccade offset indicated in red. This open-loop period is substantially shorter than the 20-100ms period examined in humans. It was determined by the visual latency of following responses, which is discussed in results **(Figure 2A)**. From eye position traces in the open-loop period we fit a linear regression line to obtain the post-saccadic following response (PFR) vector. We then projected a PFR vector (red arrow) onto the vector representing the aperture motion (blue arrow, length indicating its distance traveled in the open-loop). Comparing the length of the PFR vector projected onto the motion vector provides an estimate of the PFR gain, and a second measure is taken for the angular error between the vectors to evaluate how accurately PFR aligned with motion direction **(Figure 1D)** To examine the time-course of motion tracking in the pre- and post-saccadic periods we projected eye velocity traces along the motion direction and divided by the stimulus speed. Thus, if the eye velocity aligns with target motion we would obtain positive values, with a value of 1 indicating exact tracking of its speed.

We controlled for any systematic drifts in eye position and in saccade landing position that were specific to the aperture locations. We found at some target locations there was a small but systematic post-saccadic drift in the eye position for individual marmosets. These systematic drifts could reflect idiosyncratic aspects of our setup for imaging the eye or its initial calibration. Though they are typically small, they could still impact our ability to infer stimulus motion from post-saccadic eye movements. In particular, the estimates of angular errors in the PFR vector would be biased towards the direction of the mean drift. Thus we applied a normalization of the PFR vector to correct for systematic post-saccadic drifts identified per aperture location. The correction was blind to stimulus motion. In each session, we computed the mean post-saccadic PFR averaging across all trials irrespective of stimulus motion for saccades to each of the six possible aperture locations, and then subtracted the mean vector for each location from the PFR vectors measured at that location **(Figure 1E)**. All statistics reported use this “corrected” PFR vector. After the PFR vector is projected onto the vector direction of stimulus motion to give a single value, the velocity gain. A positive velocity gain is indicative of smooth eye movements that are on average following stimulus motion.

We also investigate the offset in saccade landing positions to determine if they were deviated along the direction of stimulus motion. We defined a saccade end-point vector, measured as the eye position at the end of the saccade minus the center of the aperture. Like the PFR measure, we again normalized per target location for any systematic deviations in saccade landing position by subtracting the mean end-point position for each aperture location. The end-points vectors were projected onto stimulus motion. Therefore, the positive deviations represent landing along the target motion direction, whereas the negative deviations represent landing opposite from the target motion direction. Using the saccade end-point vector, we can further define an angular error for PFR, and assess to what extent they provide a reliable measure of motion direction. We then compared if using a vector sum of the direction provided by PFR and the direction provided by saccade endpoints would give an improved estimate of stimulus motion.

Results

We measured post-saccadic smooth eye movements in marmosets to test whether they could provide evidence that pre-saccadic planning influences the eyes' post-saccadic following response (PFR) as previously observed in humans (Kwon, Rolfs, & Mitchell, 2019). We examined eye movements within a simple saccade foraging task that required minimal training **(Figure 1A)**. In each trial, the marmoset was trained to maintain fixation on a central point for 100-300ms, after which three dot field motion stimuli appeared in peripheral apertures of equal eccentricity and separation from each other. Each aperture contained 100% coherent motion randomly sampled from 16 motion directions spaced equally around the circle. The marmoset responded by making a saccade to one of the three apertures immediately after stimulus onset. To encourage foraging between different locations across trials, a juice reward was delivered if the marmoset selected an aperture that differed from that selected in the previous trial. We found that during initial task piloting, marmosets worked larger trials counts when sampling between three instead of two locations, and thus opted for that configuration throughout our experiments. The target apertures were presented in two different spatial configurations across blocks of 20 trials. The first configuration was a triangle with an upwards point and two lower base targets, and the second was flipped vertically.

Marmosets completed several hundred saccade trials in daily sessions. In some sessions the marmoset was allowed to work up to 600 trials using stimuli with unlimited lifetime dots (6.75 dva/sec). In those sessions they completed an average of 394 saccade trials (sd. 133) that met our criteria for obtaining accurate initial fixation (1.5 dva fixation window) and making a saccade within the target aperture (see methods). In other sessions testing other stimulus conditions they were allowed to work up to 1200 trials (unlimited and limited lifetime dots interleaved, 12 dva/sec). In those sessions they completed on average 876 (+/- 205 sd.) saccade trials. To include saccade trials in subsequent analyses, we excluded any trials if there was a double-step saccade into the target aperture or if there was a corrective saccade within 200 ms after landing inside the aperture (see methods). This removed on average 9.9% (+/- 3.5% sd.) of the total trials, giving on average of 355 and 789 included trials from 600 and 1200 trial sessions.

Marmosets learned to forage between the three apertures with varied location biases. Each marmoset exhibited different average completed trials counts for each of the six possible aperture locations **(Figure 1B, light-filled regions)**. Marmosets 1 and 4 preferred right spatial targets while marmosets 2 and 3 avoided targets at the vertical meridian. And although marmosets were rewarded for selecting a different aperture in consecutive trials, they often made a saccade back to the same location, especially if the target aligned with their spatial bias (**Figure 1B, dark-filled regions**). We find that on average they made 35.3% (range 32-40) return saccades. Further analyses included all trials regardless of whether or not they involved a relapse to a previous location.

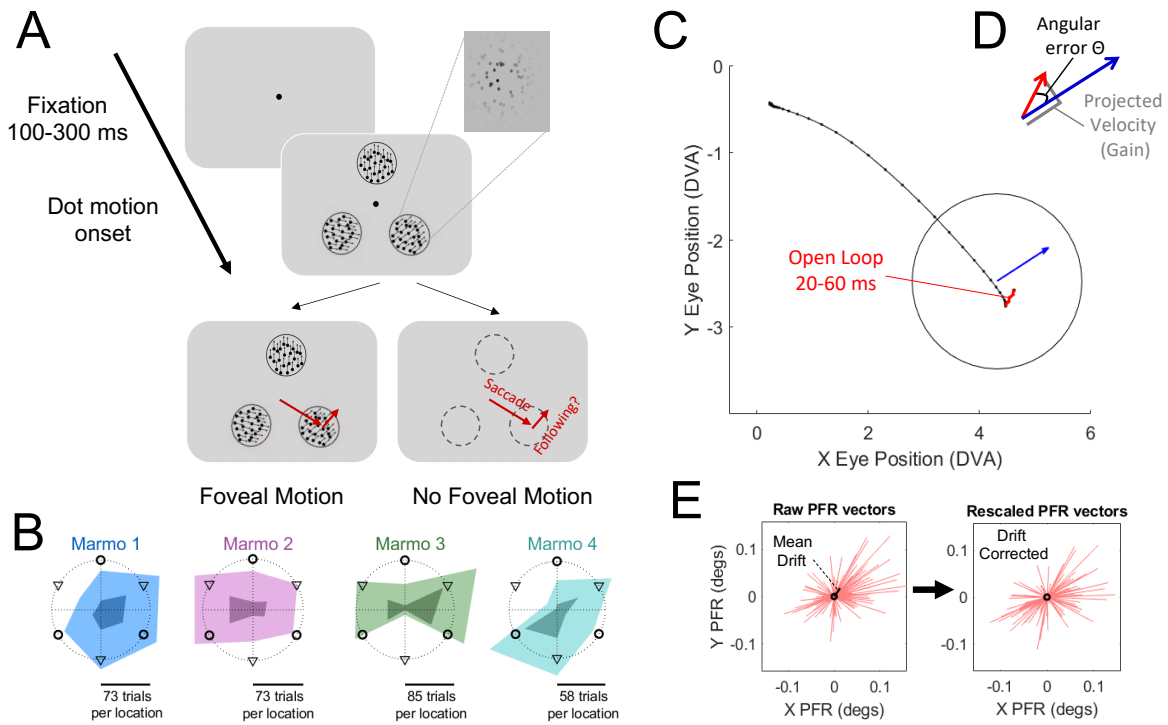

Figure 1. Experimental paradigm and marmoset behavior. ***(A)*** *For each trial, the marmoset held fixation for 100-300ms after which it was presented with three equally eccentric motion apertures. Dot-motion apertures contained 100% coherent motion sampled independently from 16 directions. Each aperture had a Gaussian window overlay. We rewarded saccades to any aperture as long it differed from the previous trial to encourage foraging. In 50% of trials, the dot motion stimuli disappeared during saccade flight such that no stimulus motion was ever presented foveally (i.e., Foveal Motion vs. No Foveal Motion).* ***(B)*** *Marmosets exhibited different spatial biases for average trials completed as a function of the size aperture locations (indicated by the lighter filled regions). They also performed a significant fraction of return saccades to a location chosen in the previous trial (indicated by the darker filled regions).* ***(C)*** *The 2D traces of eye position from a single trial demonstrate a drift along the target motion during the open loop from 20-60 ms following saccade offset. The black dots represent raw eye-position samples from the eye tracker. The eye position began within the fixation window and jumped to the target aperture (indicated by the black open circle). Eye position during the open-loop is indicate in red. Eye position drifts along the same direction as the stimulus motion in the aperture although with reduced amplitude relative to the actual dot displacement of the stimulus (indicated by the blue arrow).* ***(D)*** *Two measures of following were computed, the PFR gain which is the projection of the PFR vector (in red) along motion direction and the PFR angular error which is the difference in direction between the PFR and motion vector. The blue arrow depicts the vector for target motion, while the red arrow depicts the PFR vector for this trial. E) We corrected for any mean drift per aperture location that would have biased PFR vectors. The left plot indicates the raw PFR vectors across a single example session in red, with the mean drift potted in black. The right plot indicates the rescaled PFR vectors after subtracting away the mean drift for that location.*

We found that average eye position tracked the target motion immediately following saccade offset. As illustrated for an example trial **(Figure 1C)**, the 2D eye position demonstrates a small drift after saccade landing in a peripheral aperture. We projected the 2-D drift in eye position onto the stimulus motion vector in the target aperture (shown as the blue vector). To measure the degree of following in each trial we computed the PFR gain, defined by the shift in eye position during the open-loop period (20-60 ms) after the saccade **(Figure 1D)**. The open loop period was defined from 20-60 ms to 1) avoid contamination from saccadic transients within 20ms of saccade offset, and 2) eliminate the influence of post-saccadic motion at the fovea from driving following at a visual delay, which we estimated no shorter than 60ms (see methods). In the example trial shown, the drift in eye position during the open-loop period (shown in red) follows a similar direction as the stimulus motion (indicated by the blue vector). The amplitude of the drift is reduced relative to stimulus motion over that period, reflecting a low 10-20% gain in following. For each trial, we computed the PFR gain by projecting the PFR vector onto the motion vector and normalizing it by the speed. A PFR gain of 1 would indicate matched speed to the target motion whereas a negative value reflects eye velocity in the opposite direction.

We also consider how accurately the PFR vector aligned with the target motion defined by the angular error in each trial **(Figure 1D)**. The angular error is the difference in angle (irrespective of amplitude) between the PFR vector and target motion vector, wherein values near zero indicate better alignment in following. One issue with the angular error as a measure is that it is very sensitive to mean drift in eye position after saccades. Although small, we did observe at some aperture locations there was a mean post-saccadic drift that was independent of stimulus motion **(Figure 1E)**. This drift might reflect idiosyncratic aspects of our eye imaging or calibration that vary across locations on the screen. We corrected for mean drift in subsequent analyses by subtracting it, per aperture location, from the PFR vectors before computing the PFR gain or angular error.

Marmoset monkeys exhibit comparable PFR gain and saccade end-points as humans.

The time-course of eye velocity exhibited a low gain following response for stimulus motion that was present both in pre- and post-saccadic periods **(Figure 2A-B).** We compared the time-course to that found among human participants in a previous study (Kwon et al, 2019). The human study included only two motion directions, either clockwise or counter-clockwise running tangent to the center-out saccade. The speed of the moving dots was 6.75 dva/s for both human and marmoset studies. To aid in comparison, we begin our analyses restricted to cases where stimulus motion was within 45 degrees of tangent to the saccade. When time-locked to the stimulus onset, the average projected velocity shows an increase from zero to low-gain following of roughly 5% gain at a visual delay of 60 ms **(Figure 2A)**. We superimposed the average velocity gain for three conditions: the first in which the motion stimulus remained present after the saccade (in red: foveal motion), the second in which the motion stimulus disappeared in saccade flight (in blue: no foveal motion), and the last in which velocity was projected onto the motion of one of the other apertures instead of the saccade target (in black: other stimuli). All three conditions showed a nearly equal low 5% velocity gain before the

saccade. Immediately after the saccade, PFR gain diverged to favor the target motion over the other aperture motion (**Figure 2B, red/blue curves vs black curve**). The drive for the motion of other apertures remained low and gradually decayed, but for the target motion it abruptly increased in the open-loop period. The gain during the open-loop period was indistinguishable for target motion regardless if the stimulus remained (red) or disappeared (blue) in saccade flight, reflecting the presence of foveal motion did not yet make a difference due to the visuo-motor delay. However, after the open-loop period the velocity gain diverges with the presence of foveal motion driving a stronger PFR gain (red) and otherwise decay without foveal motion (blue). The divergence at 60 ms is consistent with our estimate of visuo-motor delay from stimulus onset (Figure 2A) and previous estimates for ocular following (Cloherty et al, 2020).

The PFR gain averaged in the open-loop period reflected a 10-15% following response in both marmosets and humans (**Figure 2C**). We projected the PFR vector from the open-loop period onto the target motion for each trial, normalized by target speed, and averaged across trials to estimate PFR gain for each participant. Humans showed an average PFR gain of 13.2% which compared closely to 10.4% in marmosets (Human: $t=4.26, df=7, p=0.0037$; Marmoset: $t=21.36, df=3, p=0.0002$). A two-way ANOVA revealed no significant main effects for the difference between foveal versus non-foveal motion ($F(1,20)=0.06, p=0.81$), for differences between human versus marmosets ($F(1,20)=0.76, p=0.39$), nor was there any interaction ($F(1,20)<0.01, p=0.94$). Examining the average velocity traces per marmoset, the time-course was consistent across the four marmosets (**Figure 2E, color traces**), and followed a similar qualitative pattern as that seen in humans (**Figure 2E, black traces**). Velocity traces overlapped for foveal vs non-foveal motion in the open-loop period (foveal motion/ solid lines; no foveal motion/ dotted lines) but then diverged after with foveal motion increasing the gain and otherwise decaying without foveal motion. The main difference between humans and marmosets was the duration of the open-loop period, which in marmosets concluded at 60 ms (shaded area) as opposed to 100 ms in humans (horizontal black line), due to their longer visuo-motor delay.

There were also systematic shifts in the saccade end-points along the target motion direction **(Figure 2D)**. We computed the saccade landing point by measuring the raw (unsmoothed) eye position at the saccade offset relative to the center of the target aperture. As with the PFR gain, the saccade end-points were projected onto the target motion axis to provide a single value for the deviation (in degrees of visual angle, dva). Positive deviations reflect deflections along the target motion axis. The saccade end-points were on average 0.21 dva in humans which was comparable to 0.18 dva in marmosets (Human: $t=7.37, df=7, p=0.00015$; Marmoset: $t=8.61, df=3, p=0.0033$). A two-way ANOVA revealed no significant differences between foveal and non-foveal motion in the saccade end-points ($F=0.01, df=(1,20), p=0.93$), differences between human versus marmosets ($F=0.88, df(1,20), p=0.36$), nor was there any significant interaction ($F=0.16, df(1,20), p=0.69$). Marmosets show deviations in saccade end-points along the target motion axis comparable to humans.

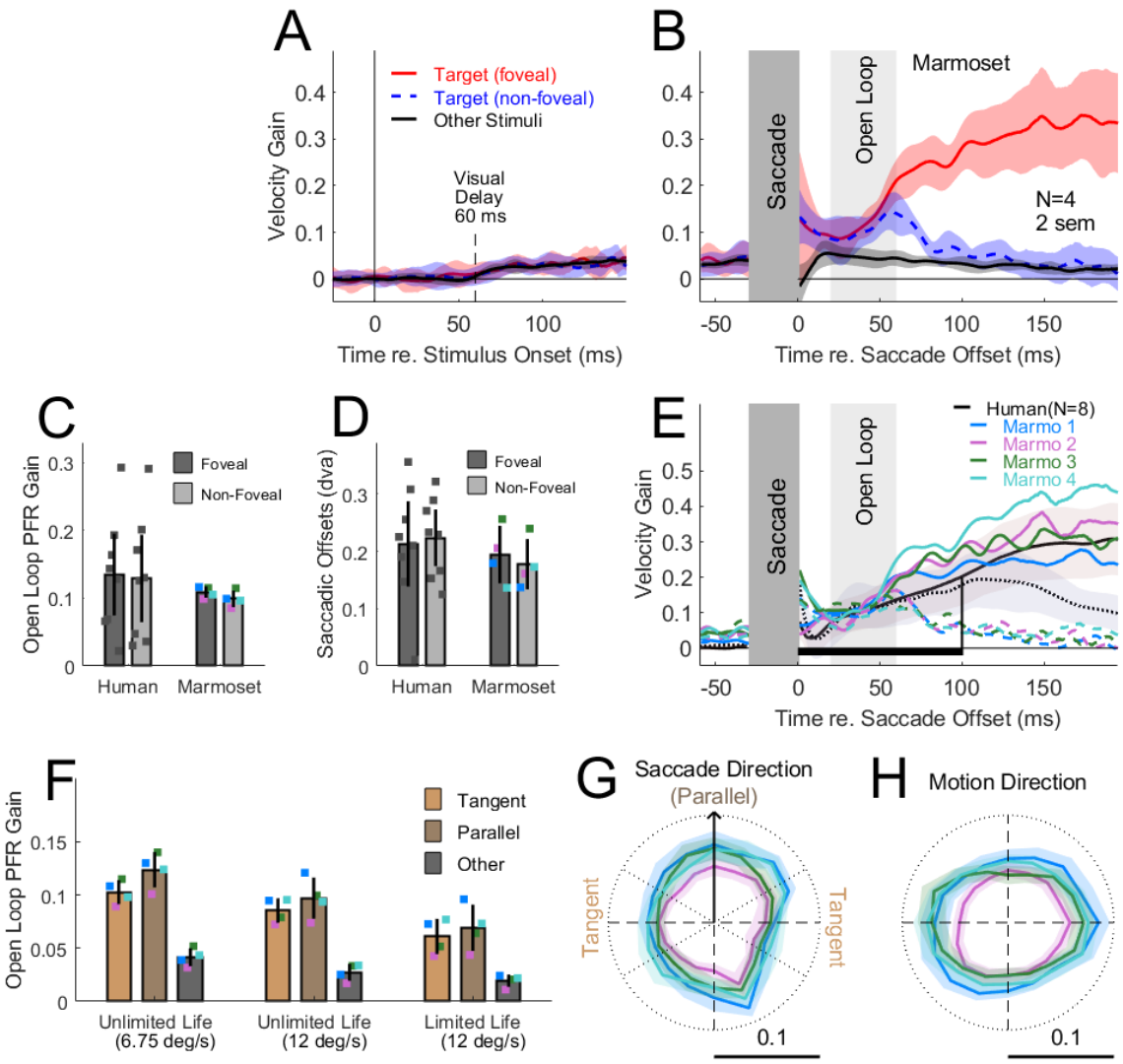

Figure 2. Post-saccadic following response (PFR) and saccade end-points tracked target motion for both humans and marmosets. ***(A)*** *The mean eye velocity gain projected along the target motion axis is shown across 4 marmosets aligned to the stimulus onset. Again, values of one reflects matched following with target motion while zero would indicate no systematic following. Three conditions are shown: the first in which the stimuli were still present upon landing (red; foveal motion); the second in which stimuli were absent upon landing (blue; no foveal motion), and the third in which velocity gain was measured relative to motion in other apertures than the saccade target (black: other stimuli). Error bars represent 2 SEM across subjects.* ***(B)*** *Mean eye velocity traces aligned to the saccade end-points (same conventions as in panel A). We focused subsequent PFR analysis on the open-loop interval from 20 to 60ms after the saccade. The velocity traces during the saccade transient are occluded (shaded in dark gray).* ***(C)*** *The PFR gain in the open loop period across humans and marmosets with individual dots representing each participant. Colored dots indicate individual marmosets. Error bars are 2 SEM.* ***(D)*** *The saccade end-points along target motion across humans and marmosets (same conventions as in panel C).* ***(E)*** *Velocity gain traces over time for individual marmosets (in color) and the mean from humans (N=8, black). Solid traces represent velocity gain when the stimulus is present after the saccade (foveal motion) and dotted traces when absent (no foveal motion). The shaded region marks the open-loop period (20-60ms) and the*

black horizontal bar the open-loop period in humans (20-100ms). ***(F)*** *Comparison of the PFR gain during the open loop period in marmosets across different speeds and dot lifetime conditions are broken out based on the target motion being tangent (yellow) or parallel (brown) with the center-out saccade, or for the case of the motion in other apertures than the saccade target (black). Error bars are 2 SEM.* ***(G)*** *The PFR gain averaged across limited lifetime dots at 12dva/sec are shown as polar plots broken out by the target direction expressed relative to the center out saccade direction (indicated by the upward black arrow). Across marmosets the gain was similar for motion that was parallel or tangent to the saccade axis with a bias for larger gains along the axis of the saccade.* ***(H)*** *Polar plots of PFR gain broken out by target motion reveal a bias for stronger gains with horizontal motion. Error bars are 2 SEM in G-H.*

PFR generalizes across a full range of motion directions and to limited lifetime dot fields

The PFR generalizes across a full range of motion directions as well as other stimuli, including limited lifetime dot stimuli. The previous study in humans (Kwon et al, 2019) focused on stimulus motions that were orthogonal to the saccade vector (clockwise or counter-clockwise) in order to reduce the possible impact of saccade transients on velocity. Although saccades produce a large velocity transient along directions parallel to the saccade, we reduced that possible contamination in velocity by eliminating the first 20 ms after the saccade offset from analyses in our definition of the open-loop period. Thus, we may be able to measure PFR reliably across a range of motions spanning 360 degrees. We pooled foveal and non-foveal motion trials and instead split the data into halves where aperture motion ran within 45 degrees parallel (yellow) or 45 degrees tangent (brown) to the saccade **(Figure 2F left)**. Further, we quantified how PFR gain for motion in the target aperture compared to the gain for the motion of the other non-target apertures (in black). Considering only unlimited life dots at 6.75 dva/sec (**Figure 2F, left**), we found that the gain was similar for parallel or tangent motion relative to the saccade direction, and in fact, smaller gain for the tangent than parallel motion case (10.2% vs. 12.4%; t=6.41,df=3,p=0.0077). The gain for motion from the other aperture was only 4.1%, significantly smaller than either tangent or parallel motion for the target (Tangent: t=18.61,df=3,p=0.0003; Parallel: t=16.63,df=3,p=0.0004). PFR is thus robust across a range of motion directions, and further, comparison of gain for the saccade target as opposed to other apertures.

We also found that PFR gain was observed with limited lifetime dot stimuli and stimuli moving at higher speeds. We tested three different types of stimuli: unlimited lifetime dots with a speed of 6.75 dva/sec, and unlimited and limited lifetime dots with a speed of 12 dva/sec (**Figure 2F, horizontal axis**). A two-way ANOVA revealed a main effect for the type of stimulus ($F(2,27)=23$, $p<0.0001$), as well as an effect for motion type being parallel, tangent, or for the other aperture ($F(2,27)=74.8$, $p<0.0001$), and no significant interaction ($F(4,27)=1.39$, $p=0.26$). Pooling across stimulus types, there was no significant difference between tangent and parallel target motion with an average gain of 8.3% and 9.6% respectively (t=2.94,df=3,p=0.06), but the gain of the other aperture motion was still nearly three times smaller at 2.9% than either of them (Tangent: t=14.1,df=3,p=0.0007; Parallel: t=9.67,df=3,p=0.0023). At 12 dva/sec the limited lifetime dots produced a smaller average PFR gain than unlimited lifetime dots (mean 6.5% vs 9.1%; t=9.33, df=3, p=0.0026). The gain was marginally smaller at 12 dva/sec as compared to 6.75 dva/sec

with unlimited lifetime dots (mean 9.1% vs 11.3%; t=3.77,df=3, p=0.0325). However, the PFR gain was still significant with limited lifetime dots at 12 dva/sec with an average of 6.5% for target motion (pooling parallel and tangent, t=7.12, df=3,p=0.0057) and lower gain of 1.9% for other aperture motion (t=6.74,df=3, p=0.0066). These results suggest that PFR is robust for use with limited lifetime dot stimuli, and thus could be used when testing stimulus reliability.

PFR was relatively uniform in magnitude when broken out as a function of how target motion aligned with saccade direction. We examined this possibility for the limited lifetime dot stimuli. Across the four marmosets, we found that PFR gain was largely uniform although with a bias favoring gain along the saccade direction (**Figure 2G**). We also considered if the magnitude of gain might differ based on the motion of the stimulus itself. Indeed, across the four animals there was a bias for horizontal motions to have higher PFR gain than vertical motion (**Figure 2H**). But despite these biases, the PFR gain was positive across a full range of directions and thus might provide a reliable read-out of the stimulus motion based on the PFR vector.

Trial-by-trial read-out of stimulus motion direction PFR direction

Whereas the PFR gain measures the drive of motion on eye velocity, we also sought to measure how accurately motion direction can be read-out on a trial-by-trial basis. Therefore, we examined the distribution of angular errors of the open-loop PFR vector, where clustering near zero indicates alignment with target motion. As illustrated for a single behavioral session, there can be a strong correlation between the motion direction of the target and the direction recovered from the PFR vector **(Figure 3A, black)**. We can also compare the trial-by-trial PFR direction against the motion in the other non-selected apertures. For the same session we observe a weak correlation between the PFR direction and motion direction of the other apertures **(Figure 3B, grey)**. The distributions of angular error reflect tighter clustering around zero for reading out target motion (black) as compared to a broader distribution of errors for other aperture motion (grey) **(Figure 3C)**. We fit a maximum-likelihood estimate of a Von Mises distribution to the error distributions (solid lines). Averaging the error histograms across sessions for each of the four marmosets we observe a consistent pattern in which clustering around zero is narrower for the target aperture motion **(Figure 3D)**. Marmosets did differ in the strength of clustering, with marmosets 1 and 4 showing tighter distributions for the target.

To quantify the degree of clustering in angular errors we computed the median of the absolute value of angular errors, which we term the median PFR error. For the example session (Marmo 1), the PFR direction provided a relatively accurate estimate of target motion with a median error of 27.4 degrees, whereas for the other aperture motion the median error was 79.5 degrees, close to chance which is at 90 degrees and would be reflected by a flat distribution from -180 to 180 degrees. Averaging across sessions for each animal, we find the median PFR error was 42.6 degrees (+/- 11.6 sd.) for target motion across animals as compared to 76.1 degrees (+/- 3.0 sd) for other aperture motion (**Figure 3F, left**). The same analyses can also be

applied to saccade end-point vectors (see methods). We find that saccade end-points, like PFR, carry more information about target motion than other aperture motion, with a median error of 44.9 degrees (+/ 7.5 sd.) as compared to 92.8 degrees (+/- 3.6 sd.) (**Figure 3F, middle**). A two-way ANOVA comparing factors of PFR vs saccade end-points and target vs other aperture motion revealed a main effect for PFR vs saccade end-points ($F(1,12)=6.97$; $p=0.0216$), a main effect for target vs. other aperture motion ($F(1,12)=125.09$; $p<0.0001$), and no significant interaction. The median error was smaller for the target than other aperture motion by 44.0% for PFR ($t=6.85, df=3, p=0.0064$) and by 51.6% for saccade end-points ($t=9.97, df=3, p=0.0021$). In the case of target motion the PFR errors were not significantly better than errors from saccade end-points ($t=0.57, df=3, p=0.6065$), but read-out of the other aperture motion was improved with 18% smaller errors for PFR compared to saccade end-points ($t=6.74, df=3, p=0.0067$). In fact, the information for other aperture motion among saccade end-points was no better than chance ($t=1.56, df=3, p=0.2158$). Both PFR and saccade end-points contribute information about target motion on a trial-by-trial basis in the open-loop period, but there is much less information about other aperture motions. The distribution of information reflects a preferential weighting for the target aperture motion in influencing both PFR and saccade end-points during pre-saccadic attention.

Combining PFR and saccade end-points *estimates does not significantly improve angular errors*

Finally, we considered to what extent the PFR and saccade end-points might provide estimates with independent sources of error, and if independent, if they could be combined to provide a better estimate of stimulus motion. To quantify the degree of their correlation we took the unit vectors for each type of angular error (PFR and saccade end-point angular error) and computed the coherence. As these are circular variables, coherence is the appropriate measure of correlation, and will give a positive magnitude when there is a significant linear relationship with the phase representing how well they align. On average, the magnitude of coherence was modest for errors related to target motion with a mean value of 0.073 (+/- 0.039 sd.), and only 6 of 30 sessions reached an individually significant value ($p<0.05$). For errors related to other target motions, however, there were significant correlations with a mean coherence of 0.204 (+/- 0.094 sd.) and 29 of 30 individual sessions reaching significance ($p<0.05$). For those sessions showing significant correlation, the phase was clustered near zero (6.8 +/- 19.2 sd. degrees), indicating an alignment in the errors. This suggests that PFR and saccade end-points may provide information with independent sources of error for target motion but not the other aperture motion, which could impact whether or not combining them yields a superior estimate.

A vector sum taken between PFR and saccade end-points produced only modest improvements for estimating target motion and gave a modest impairment for the other aperture motion. For the example session shown previously, the vector sum produced tighter clustering in its angular errors than either PFR or saccade end-points (**Figure 3E**). Averaging across sessions confirmed a modest improvement for the vector sum error at 36.6 (+/- 11.6 sd.) degrees as compared to the PFR error at 42.3 (+/- 8.2 sd.) degrees (**Figure 3F, right)**. By contrast, the other aperture motion showed the opposite trend with a larger average error for the vector sum

at 84.4 (+/- 2.9 sd.) degrees as compared to 76.1 (+/- 3.0 sd.) degrees for PFR. A two-way ANOVA, however, indicated these trends were not significantly different between the PFR and saccades end-points (F(1,12)=0.13; p=0.7282), and failed to reach statistical significance (F(1,12)=3.59; p=0.0826). As the vector sum produced only modest changes in read-out, we choose to focus on the single measure, the PFR angular errors, in further analyses. We were interested in how its performance might compare against explicit saccadic reports.

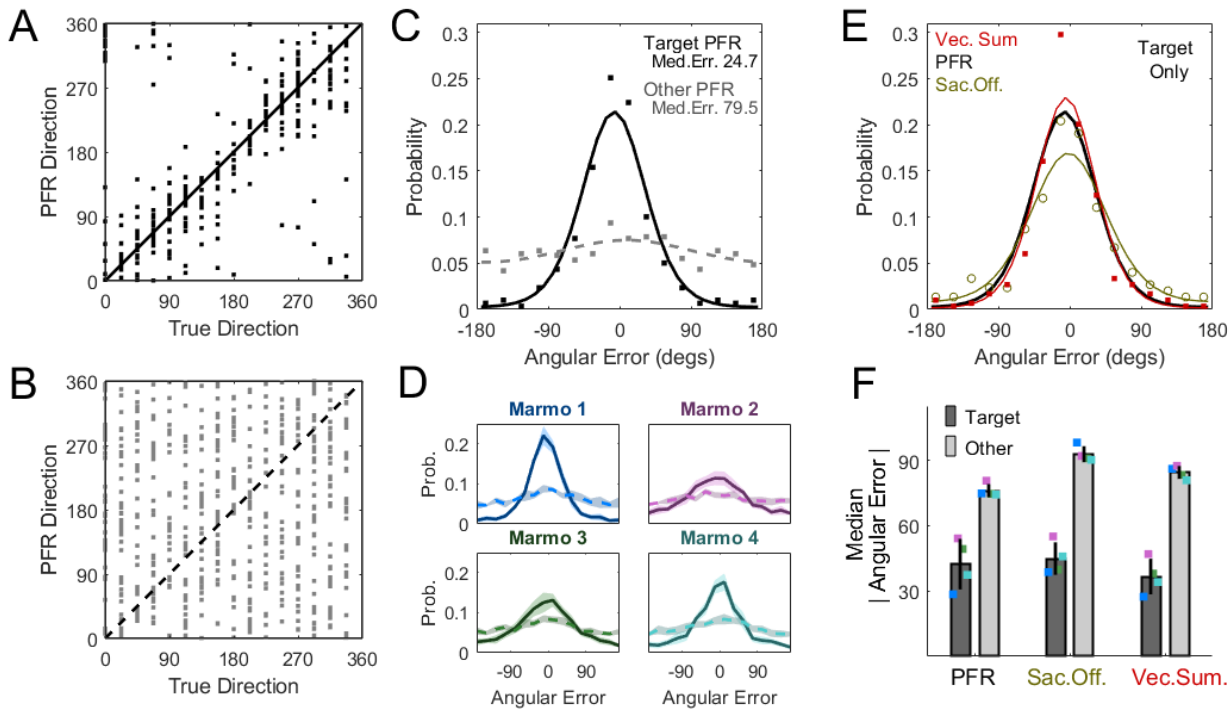

Figure 3. PFR angular error in an example session and across individual subjects. *Distributions of angular errors are shown for a single session from Marmoset 1 in A-C and E.* ***A)*** *The direction of motion in the saccade target aperture is plotted against the PFR vector direction (black points indicate individual trials). B****)*** *The direction for the other non-saccade targets against the PFR direction is shown (grey points indicate single trials).* ***C)*** *The probability histogram of PFR angular errors for the saccade target (black) and the other non-selected apertures (grey-dotted) is shown for the same session. Both distributions were fit with a Von Mises function.* ***D)*** *Average angular error distributions from the target (solid lines) and other aperture (dashed lines) for individual marmosets.* ***E)*** *The probability distribution of PFR angular errors for saccade target motion (black), compared against the angular errors from saccade end-points (gold), and from combining the two to form a vector sum measure (red), overlaid with Von Mises fits.* ***F)*** *The median angular errors for PFR, Saccade end-points , and the vector sum for target motion (dark grey) and other non-selected aperture motion (light grey). Individual marmosets are indicated by colored squares. Error bars are 2 SEM.*

Angular errors from PFR provide roughly half the accuracy of intentional saccadic reports

A previous study examined the distribution of angular errors from saccadic reports made in an analog motion estimation task using limited lifetime dots (Cloherty et al., 2019). They trained two marmosets to view a centrally presented motion dot field at the fovea and make an analog report of its motion by a saccade to the location extrapolated from the central motion to a

peripheral surrounding ring. They also varied the signal strength of motion in the dot fields by adjusting the bandwidth of the distribution from which dot directions were drawn, ranging from all dots having a uniform direction (signal strength of 1), to them being drawn over a range of +/- 90 degrees around a mean direction (signal strength of 0.5), or completely at random (range of +/- 180 degrees giving a signal strength of 0). They quantified the distribution of angular errors in the reported motion direction by fitting an adjusted Gaussian that included a lapse rate across signal strength (see methods, Cloherty et al, 2019). In three of our four marmosets we were able to perform additional experiments to measure the PFR across different signal strengths and fit the angular error distributions using identical methods.

The PFR shows a decreasing error with increasing signal strength that is comparable to saccadic reports but has about half the accuracy. The fitted angular standard deviations from the saccadic reports decreased with increasing signal strength reaching an average accuracy of 19.1 (+/- 1.7 sem) degrees in width (**Figure 4A, black and grey**). The PFR errors from the three marmosets we were able to compare also decreased with signal strength but only reached a peak accuracy about half as good (**Figure 4A, color traces**). The angular standard deviation at peak signal strength was 43.4 (+/- 2.3 sem) degrees, significantly worse than saccadic reports (unpaired t=9.38,df=3,p=0.0026). Thus, while PFR provides an automatic read-out for target motion that can be obtained with minimal training, it is substantially less accurate.

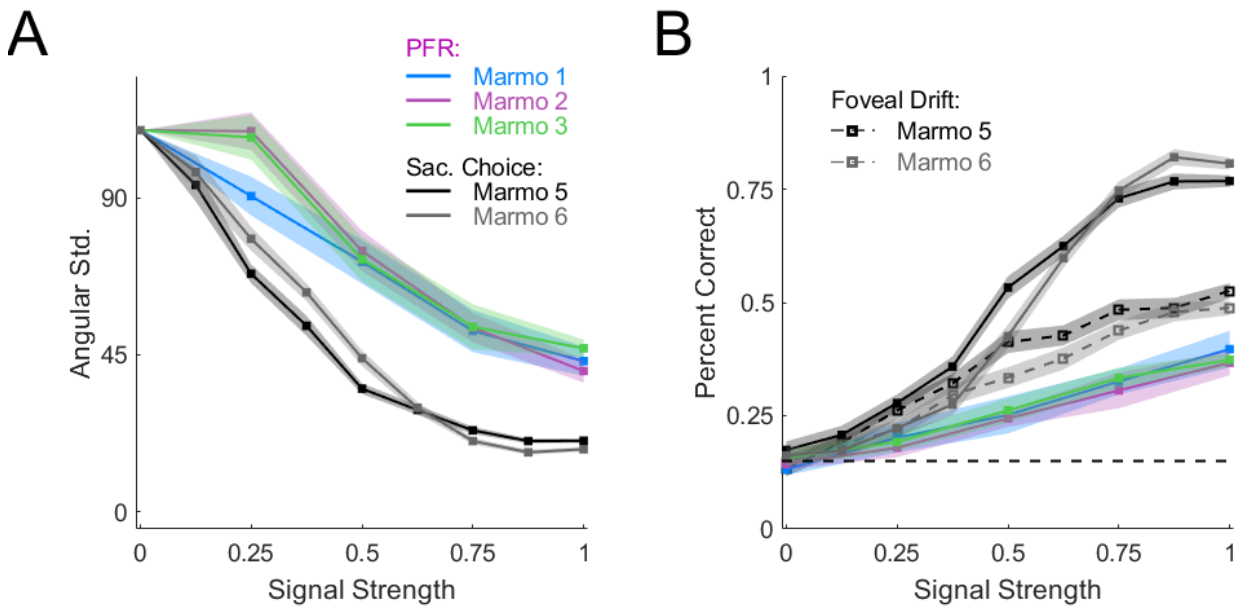

Figure 4. PFR angular errors provide about half the accuracy of a trained analog saccadic choice. ***A)*** *The angular standard deviation narrows across signal strength (motion coherence) for PFR in our three untrained animals (blue, purple, green). By comparison saccadic motion reports are roughly twice as accurate across signal strength (black, grey) in two marmosets (reproduced from Cloherty et al., 2019). Error bars are 2 SEM.* ***B)*** *The accuracy of PFR and saccadic choices are replotted from A in terms of task performance with correct choices defined as being within 45 degrees of the true stimulus direction (same color conventions). In the two marmosets providing saccadic reports (marmosets 5,6) we additionally measured the following response after the onset of a foveal motion stimulus at fixation (Foveal Drift: dotted lines, black, grey and can determine its accuracy as a report (dotted lines, black, grey). Error bars are 2 SEM.*

The second measure of accuracy relates to the proportion of correct choices in a task, which unlike the standard deviation of angular errors in the fitted distributions above, also includes errors due to lapses. The previous study defined correct choices as having an angular error of less than 27 degrees, which in the task resulted in a juice reward. The percentage of correct trials increased with signal strength for saccadic reports, and consistent with angular standard deviations, was more accurate than PFR (**Figure 4B**). The peak performance was 78.7% (+/- 2.7% sem.) correct for saccadic reports as compared to 37.9% (+/-1.1% sem.) correct for PFR, a significant difference (t=21.97,df=3,p=0.0002). Thus, saccadic reports remain more accurate even when lapse rates are included.

The previous study provides a further point for comparison, as it also measured the accuracy of read-out for smooth eye movements that resemble the PFR. They found that prior to the saccade to the peripheral ring to report motion direction, there was also a drift in eye position along the direction of centrally presented motion, which they termed “foveal drift” (Cloherty et al, 2019). The foveal drift is a similar involuntary smooth eye movement as the PFR, except that it is generated by a foveal as opposed to a peripheral stimulus. Like the PFR, the foveal drift was less accurate than the saccadic reports having a mean proportion correct of 50.7% (+/- 2.6% sem) (**Figure 4B, dotted lines**), which was significantly worse (unpaired t=10.41, df=2,p=0.0091). However, the foveal drift was not identical to PFR either. It provides on average 33.7% better performance than the PFR (unpaired t=6.98, df=3,p=0.0060). In summary, saccadic reports provide the highest accuracy for reporting motion in comparison with following movements, and among following movements performance is superior for foveally presented stimuli.

Discussion

In the current study, we established that like human participants, marmoset saccades to peripheral motion apertures result in smooth post-saccadic following responses (PFR) that tracked stimulus motion at a low gain (Kwon et al. 2019). This PFR persisted even when the motion stimulus was removed in saccade flight, thus isolating the pre-saccadic contribution of motion integration from post-saccadic viewing of the stimulus at the fovea. We found that we could also isolate the component of post-saccadic following that was due to pre-saccadic motion integration by focusing our analyses on the open-loop period, an epoch before post-saccadic visual information can influence the eyes. In marmosets this epoch concluded at a visuo-motor delay of 60 ms, whereas in humans it extended out to 100 ms. In that open-loop period, we find that following responses are preferentially driven by the motion in the aperture targeted by the saccade with a 10-15% gain, whereas motion from other non-selected apertures has a much weaker influence at or below 5% gain. There was no evidence for preferential weighting to target motion in following movements prior to the saccade. Rather there was a weak gain (<5%) equally distributed across all apertures. The change in weighting of stimulus motion immediately after the saccade thus reflects the attentional selection of the target, and in future studies, could provide a behavioral index of pre-saccadic attention. Following movements also provide a behavioral read-out of the target motion direction, which though about half as accurate as an explicit saccadic report, provides motion information without the need for extensive task training.

One main difference between marmosets and humans was the brevity of their open-loop period. Kwon et al. (2019) used an “open-loop” period (20-100ms) after the saccade offset to examine the effect of peripheral motion on the PFR in humans. We found that the visual latency of the following response was much shorter in the marmoset, with a low gain following initiating after motion stimulus onset around 60ms. This value is roughly consistent with a 70 ms delay reported in an earlier study examining drift in response to foveally presented motion stimuli (Cloherty et al, 2020). This visuo-motor delay was confirmed by the latency at which post-saccadic following responses diverged for motion stimuli that remained present after the saccade as opposed to those that disappeared in saccade flight, with continued motion driving strong following with a latency around 60 ms. By comparison, the earlier study in humans did not observe significant divergence between these conditions until after 100 ms (Kwon et al, 2019). The disparity in the visual latency delay between humans and marmosets presumably arises from the differences in visual processing time due to brain size and their visual system.

The current study employed a saccade foraging task which required minimal training. These findings thus demonstrate that the PFR generalizes to less stringent task and stimulus conditions. In the earlier human task (Kwon et al., 2019), participants were cued where to make a saccade by a flashed line at fixation. Marmosets in the present study could perform a saccade to any of the peripheral apertures with no explicit cue and would receive reward as long as they explored different apertures from trial to trial. Our results confirm that PFR can be measured under these more natural, foraging task constraints.

Additionally, the former study (Kwon et al, 2019) examined a restricted set of peripheral motion directions. Our study extends those results to a full range of motion directions. The former study had tested only two directions that were tangent to the direction of the center out saccade. That design was intended to minimize interference from velocity transients caused by the saccade itself that could impact eye velocity in the open loop period. We controlled for those transients by only analyzing smooth movements 20 ms after the saccade offset. We find that it is indeed possible to measure the PFR across a full range of motion directions, and that gain is equal or slightly stronger for directions parallel to the saccade rather than reduced due to saccade contamination. We also tested that the PFR generalizes to limited lifetime dot stimuli, which are valuable for examining variations in stimulus signal strength. Together, the use of limited lifetime dots and the ability to test a full range of motions suggests that PFR could be useful as an analog read-out of motion direction for peripheral stimuli in neurophysiology studies.

A previous study trained marmosets to perform an analog motion estimation task in which the perceived direction of a foveally-presented motion stimulus was reported (Cloherty et al., 2020). Comparing the motion direction reported from PFR to that study, we found the accuracy to be only about half as good as an explicit report. It is uncertain if that accuracy would be sufficient to assess correlations with activity at the neural level. We also compared the accuracy of PFR for peripheral motion apertures to following movements for foveal stimuli. The former study found drifts at fixation during the presentation of foveal motion fields, which they termed foveal drift (Cloherty et al., 2020). We found that foveal drift, though inferior to the accuracy of saccadic reports, was still more accurate than PFR for peripheral motion stimuli. This may simply reflect that foveal motion is more strongly weighted in following movements than peripheral information. A recent neurophysiology study indicates the selective weighting of foveal

information in smooth eye movements (Mukherjee et al. 2017). In summary, the accuracy provided by the PFR appears limited both relative to saccadic reports, but also other more direct measures of following that exploit foveal stimuli. However, there are other advantages of the PFR that could mitigate the concern about its accuracy. While marmosets did learn to perform this saccadic report task, they would typically complete only 100-200 trials in daily sessions (Cloherty et al, 2020). The PFR task can yield between 700-800 accurate saccade trials in a daily session, which could provide larger numbers of repetitions for neural studies.

The PFR likely relies on different neural pathways to read-out motion information than perception. It is well established that smooth eye movements can be disassociated from the perception of motion (Spering and Gegenfurtner, 2007; Spering et. al., 2011; Spering and Carrasco, 2012). Smooth eye movements are more directly influenced by retinal motion whereas perception considers contextual factors. It appears that PFR, as a smooth eye movement, follows the same distinction from perception. A recent study from our lab investigating the recovery of motion perception in cortically-blind patients with V1 lesions found that improvements in perception did not correlate with any recovery of PFR in the blind fields, even when perception recovered to normal levels (Kwon et al., 2022). In fact, they found no significant PFR in blind-fields, suggesting that it must rely on motion signals that pass through area V1. They did, however, find some residual effect for saccade end-points retaining the bias along the direction of target motion, although much weaker than in normal controls. An open question remains if saccade end-points in the saccade foraging task might better correlate with perceptual reports. Our current results found no significant correlation between the errors in the motion read-outs for PFR and saccade end-points, which could also support a distinction between how motion information is read-out by these different measures in behavior. There is reason to suggest saccade end-points may correlate better with perception. Previous work has found that motion can bias the perceived position of peripheral targets, which in turn, biases saccade towards them (Schafer and Moore, 2007; Kosovicheva et al., 2014). Further work will be necessary to determine how read-out pathways differ from saccade end-points and the PFR during saccade foraging.

An important finding from these experiments is that PFR is also sensitive to motion from the other non-selected apertures, and thus can provide some index of pre-saccadic attentional selection based on the relative weighting of the target and other aperture information. While the former study in humans (Kwon et al, 2019) focused on PFR's relation to motion in the aperture targeted by the saccade, we additionally find that motion information is present for the other non-selected apertures. The relative influence of the target versus other aperture motion may provide a valuable metric of attentional selection. We found that after stimulus onset but before the saccade all target motions demonstrated a weak but equal gain. However, immediately after the saccade, still within the open-loop epoch, there was a preferential weighting for the saccade target. These findings demonstrate that PFR can be influenced predictively by target selection during pre-saccadic attention. This transition in weighting of stimulus information around the time of the saccade is consistent with post-saccadic enhancement found in previous studies of smooth pursuit (Gardner & Lisberger, 2001). In pursuit for selecting one of two moving dots there is a change from vector averaging before the saccade to target selection immediately after the saccade. Many studies have shown that neural responses from area MT in macaque

monkeys are predictive of the variations in pursuit behavior and that changes in gain reflect target selection (Huang and Lisberger, 2009; Lisberger, 2010). Thus, like pursuit, the PFR may provide a useful behavioral read-out to examine how fluctuations in neural activity contribute to varied motor behavior, as well as the weighting of information for selecting the target during pre-saccadic attention.

Acknowledgments

We would like to thank Dina Graf and members of the Mitchell lab for help with marmoset care and handling. We thank Shaun Cloherty for his comments on an earlier draft of this manuscript. This work was supported by NIH grants EY030998 (JFM and SC) and T32 EY007125 (SC).

References

Brainard, D. H. (1997). The psychophysics toolbox. Spatial vision, 10(4), 433-436.

Chaplin, T. A., Allitt, B. J., Hagan, M. A., Price, N. S., Rajan, R., Rosa, M. G., & Lui, L. L. (2017). Sensitivity of neurons in the middle temporal area of marmoset monkeys to random dot motion. Journal of Neurophysiology, 118(3), 1567-1580.

Cloherty, S. L., Yates, J. L., Graf, D., DeAngelis, G. C., & Mitchell, J. F. (2020). Motion perception in the common marmoset. Cerebral Cortex, 30(4), 2659-2673.

Deubel, H. (2008). The time course of presaccadic attention shifts. Psychological Research, 72(6), 630– 640.

Deubel, H., & Schneider, W. X. (1996). Saccade target selection and object recognition: Evidence for a common attentional mechanism. Vision research, 36(12), 1827-1838.

Engbert, R., & Mergenthaler, K. (2006). Microsaccades are triggered by low retinal image slip. Proceedings of the National Academy of Sciences, USA, 103 (18), 7192–7197.

Gardner, J. L., and Lisberger, S. G. (2001). Linked Target Selection for Saccadic and Smooth Pursuit Eye Movements. The Journal of Neuroscience, vol. 21, no. 6, pp. 2075–2084., doi:10.1523/jneurosci.21-06-02075.2001.

Henderson, J. M., Pollatsek, A., & Rayner, K. (1989). Covert visual attention and extrafoveal information use during object identification. Perception & psychophysics, 45(3), 196-208.

Huang, X., & Lisberger, S. G. (2009). Noise Correlations in Cortical Area MT and Their Potential Impact on Trial-by-Trial Variation in the Direction and Speed of Smooth-Pursuit Eye Movements. *Journal of Neurophysiology, 101*(6), 3012-3030.

Kleiner, M., Brainard, D., & Pelli, D. (2007). What's new in Psychtoolbox-3?

Kosovicheva, A. A., Wolfe, B. A., & Whitney, D. (2014). Visual motion shifts saccade targets. Attention, Perception, & Psychophysics, 76(6), 1778-1788.

Kowler, E., Anderson, E., Dosher, B., & Blaser, E. (1995). The role of attention in the programming of saccades. Vision research, 35(13), 1897-1916.

Kwon, S., Fahrenthold, B. K., Cavanaugh, M. R., Huxlin, K. R., & Mitchell, J. F. (2022). Perceptual restoration fails to recover unconscious processing for smooth eye movements after occipital stroke. Elife, 11, e67573.

Kwon, S., Rolfs, M., & Mitchell, J. F. (2019). Presaccadic motion integration drives a predictive postsaccadic following response. Journal of vision, 19(11), 12-12.

Li, H. H., Barbot, A., & Carrasco, M. (2016). Saccade preparation reshapes sensory tuning. Current Biology, 26(12), 1564-1570.

Lisberger, S. G. (2010). Visual guidance of smooth-pursuit eye movements: sensation, action, and what happens in between. Neuron, 66(4), 477-491.

Lu, T., Liang, L., & Wang, X. (2001). Neural representations of temporally asymmetric stimuli in the auditory cortex of awake primates. Journal of neurophysiology, 85(6), 2364-2380.

Mitchell, J. F., & Leopold, D. A. (2015). The marmoset monkey as a model for visual neuroscience. Neuroscience research, 93, 20-46.

Mitchell, J. F., Priebe, N. J., & Miller, C. T. (2015). Motion dependence of smooth pursuit eye movements in the marmoset. Journal of neurophysiology, 113(10), 3954-3960.

Mitchell J.F., Reynolds J.H., Miller CT. (2014). Active vision in marmosets: A model system for visual neuroscience. J Neurosci 34:1183–1194

Montagnini, A., & Castet, E. (2007). Spatiotemporal dynamics of visual attention during saccade preparation: Independence and coupling between attention and movement planning. Journal of Vision, 7(14):8, 1–16.

Mukherjee, T., Liu, B., Simoncini, C., & Osborne, L. C. (2017). Spatiotemporal filter for visual motion integration from pursuit eye movements in humans and monkeys. Journal of Neuroscience, 37(6), 1394-1412.

Nummela, S. U., Coop, S. H., Cloherty, S. L., Boisvert, C. J., Leblanc, M., & Mitchell, J. F. (2017). Psychophysical measurement of marmoset acuity and myopia. Developmental Neurobiology, 77 (3), 300–313.

Ohl, S., & Rolfs, M. (2017). Saccadic eye movements impose a natural bottleneck on visual short-term memory. Journal of Experimental Psychology: Learning, Memory, and Cognition, 43(5), 736.

Osborne, L. C., Hohl, S. S., Bialek, W., & Lisberger, S. G. (2007). Time course of precision in smooth-pursuit eye movements of monkeys. Journal of Neuroscience, 27(11), 2987-2998.

Osmanski, M. S., Song, X., & Wang, X. (2013). The role of harmonic resolvability in pitch perception in a vocal nonhuman primate, the common marmoset (Callithrix jacchus). Journal of Neuroscience, 33(21), 9161-9168.

Pelli, D. G. (1997). The VideoToolbox software for visual psychophysics: Transforming numbers into movies. Spatial vision, 10(4), 437-442.

Remington, E. D., Osmanski, M. S., & Wang, X. (2012). An operant conditioning method for studying auditory behaviors in marmoset monkeys. PLoS One, 7(10).

Rolfs, M., Jonikaitis, D., Deubel, H., & Cavanagh, P. (2011). Predictive remapping of attention across eye movements. Nature neuroscience, 14(2), 252.

Rolfs, M., & Carrasco, M. (2012). Rapid simultaneous enhancement of visual sensitivity and perceived contrast during saccade preparation. Journal of Neuroscience, 32(40), 13744-13752a.

Schafer, R. J., & Moore, T. (2007). Attention Governs Action in the Primate Frontal Eye Field. *Neuron, 56*(3), 541-551.

Solomon, S. G., & Rosa, M. G. (2014). A simpler primate brain: the visual system of the marmoset monkey. Frontiers in neural circuits, 8, 96.

Spering, M., & Gegenfurtner, K. R. (2007). Contrast and assimilation in motion perception and smooth pursuit eye movements. *Journal of Neurophysiology, 98*(3), 1355-1363.

Spering, M., & Carrasco, M. (2012). Similar effects of feature-based attention on motion perception and pursuit eye movements at different levels of awareness. *Journal of Neuroscience, 32*(22), 7594-7601.

Spering, M., Pomplun, M., & Carrasco, M. (2011). Tracking without perceiving: a dissociation between eye movements and motion perception. *Psychological science, 22*(2), 216-225.

Troilo D, Rowland HC, Judge SJ. 1993. Visual optics and retinal cone topography in the common marmoset (Callithrix jacchus). Vision Res 33:1301–1310.

White, A. L., Rolfs, M., & Carrasco, M. (2013). Adaptive deployment of spatial and feature-based attention before saccades. Vision research, 85, 26-35.

Zavitz, E., Yu, H. H., Rosa, M. G., & Price, N. S. (2019). Correlated variability in the neurons with the strongest tuning improves direction coding. Cerebral Cortex, 29(2), 615-626.